Advances in Nano Research, *Vol. 12, No. 4 (2022) 387-403*
https://doi.org/10.12989/anr.2022.12.4.387

Machine learning modeling and DOE-assisted optimization in synthesis of nanosilica particles via Stöber method

Hiresh Moradi*[1], Peyman Atashi[2], Omid Amelirad[3], Jae-Kyu Yang**[1], Yoon-Young Chang[1c] and Telma Kamranifard[2]

[1]*Department of Environmental Engineering, Kwangwoon University, Seoul, Korea*
[2]*Research and Development Department, Ghaffari Chemical Industries Corp., Tehran, Iran*
[3]*Department of Mechanical Engineering, Sharif University of Technology, Tehran, Iran*

(*Received November 14, 2021, Revised January 25, 2022, Accepted January 26, 2022*)

Abstract. Silica nanoparticles, which have a broad range of sizes and specific surface features, have been used in many industrial applications. This study was conducted to synthesize monodispersed silica nanoparticles directly from tetraethyl orthosilicate (TEOS) with an alkaline catalyst (NH_3) based on the sol–gel process and the Stöber method. A central composite design (CCD) is used to build a second-order (quadratic) model for the response variables without requiring a complete three-level factorial experiment. The process was then optimized to achieve the minimum particle size with the lowest concentration of TEOS. Dynamic light scattering and scanning electron microscopy were used to analyze the size, dispersity, and morphology of the synthesized nanoparticles. After optimization, a confirmation test was carried out to evaluate the confidence level of the software prediction. The results revealed that the predicted optimization is consistent with experimental procedures, and the model is significant at the 95% confidence level.

Keywords: design of experiments (DOE); machine learning; nanoparticles; silica; Stöber method

1. Introduction

Colloids have attracted the attention of many scientists because of their specific features and broad range of applications in various industrial and consumer products, including food Dickinson (2015), de Moraes *et al*. (2021), cosmetics Khezri *et al*. (2018), Moradi *et al*. (2021), catalysts Jiao *et al*. (2021), Prabha *et al*. (2021), ceramics Cerbelaud *et al*. (2016), Ma *et al*. (2021a), pigments Jiang, biomedicine Abulateefeh *et al*. (2011), Guo and Wang (2011), Shah and Rather (2021), and polymer composites Kim *et al*. (2007), Liu *et al*. (2020), Arani *et al*. (2021). According to the IUPAC definition, colloids are stable particles with dimensions in the range of 1–1000 nm suspended or dispersed in the continuous phase of different compositions or states Everett (1972). At first glance, these heterogeneous mixtures appear identical to solutions and suspensions. However, further accurate investigations imply that their intrinsic specific traits give them a distinct advantage over other heterogeneous and homogeneous mixtures. The differences between the properties of solutions, colloids, and suspensions are listed in Table 1.

As it is difficult to measure the size of the particles in the dispersed phase and since their appearance is similar to solutions, colloids are sometimes identified and characterized by their physicochemical properties. They are classified into different categories depending on their dispersed and dispersion phases, as shown in Table 2. For instance, a *sol* is a collection of stable solid colloidal particles suspended in liquid, whereas a *gel* is defined as a continuous solid skeleton enclosing a continuous liquid phase, and an *emulsion* refers to liquid drops in a liquid phase.

The critical properties of colloids have aroused scientists' enthusiasm to make a breakthrough in developing inorganic, polymeric, carbon, and composite particles (Xiong *et al*. 2020, Fu *et al*. 2021, Zhu *et al*. 2021, Liu *et al*. 2011) attempted to design monodisperse resorcinol–formaldehyde polymers and carbon spheres Liu *et al*. (2011). Furthermore, other scientists have tried to devise new methods to use these polymeric particles to increase the productivity of daily routine instruments Sun *et al*. (2021), Zhang *et al*. (2022). The use of tunable porous carbon spheres for high-performance rechargeable batteries and carbon nanotube dispersion in polymeric composites are cases in point (Tian *et al*. 2018, Bai *et al*. 2020, Ghazanfari *et al*. 2020, Li *et al*. 2020, Liu *et al*. 2020, Oyarhossein *et al*. 2020, Wang *et al*. 2020, Feng *et al*. 2021, Hu *et al*. 2021).

Among the variety of colloidal particles, inorganic particles, and specifically silica nanoparticles, have revolutionized the utilization of colloids in chemistry because of their extensive potential applications in many industries Kim *et al*. (2007), Zhang *et al*. (2016), TM *et al*. (2020), de Moraes *et al*. (2021), Prabha *et al*. (2021). Fig. 1(a) shows the number of publications from 2000 up to now, based on web of science's search result for silica nanoparticles. As it obvious in Fig. 1 the application of silica nanoparticles to improve the properties of different material, in various field of study has been increasing in last

*Corresponding author, Ph.D.,
E-mail: h.moradi@kw.ac.kr
**Co-corresponding author, Professor,
E-mail: jkyang@kw.ac.kr

ISSN: 2287-237X (Print), 2287-2388 (Online)

Table 1 Properties of solutions, colloids, and suspensions Everett (1972)

	Solutions	Colloids	Suspensions
Appearance	Homogeneous	Heterogeneous	Heterogeneous
Particle size	0.01–1 nm; atoms, ions, or molecules	1–1000 nm; dispersed large molecules or aggregates	Over 1000 nm; suspended large particles or aggregates
Effect of light	Do not scatter light	Scatter light (Tyndall effect)	May either scatter light or be opaque
Effect of sedimentation	Do not separate on standing	Do not separate on standing	Particles will eventually settle out
Extraction	Do not separate on standing	Do not separate on standing	Particles settle out

Table 2 Classification of colloids Bergna (2005)

Dispersed phase Dispersion Phase	Gas	Liquid	Solid
Gas	No such colloids are known	Liquid aerosol	Solid aerosol
Liquid	Foam	Emulsion	Sol
Solid	Solid foam	Gel	Solid sol

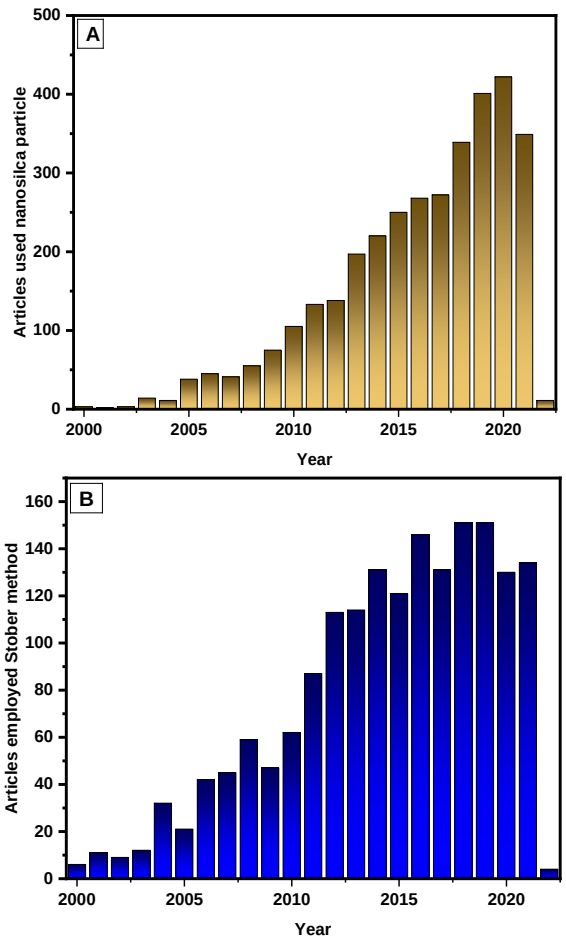

Fig. 1 (a) The number of published articles used nanosilica particle, (b) Published articles employed Stöber method in their synthesis and modification studies

decade Bai *et al*. (2021). The Stöber endeavor toward the development of monodisperse silica spheres based on the hydrolysis of tetraethyl orthosilicate (TEOS) in the presence of water in an ammonia-catalyzed sol–gel reaction paved the way for synthesizing silica particles with different sizes and shapes Stöber *et al*. (1968). After Stöber numerous researcheres have started using Stöber method in their synthesis and modification studies and it can be seen in Fig. 1(b) that, nowadays, Stöber approache has a pivotal imprtance in synthesis of silica and other nanoparticles.

It has been revealed that the chemical reactions involved in the Stöber method are divided into two main steps, hydrolysis, and condensation Svirbely and Mador (1950), van Blaaderen and Kentgens (1992), Van Blaaderen *et al*. (1992), Aelion *et al*. (2002), Curley *et al*. (2021), as depicted in Fig. 2.

The importance of controlling particle size and dispersity has encouraged researchers to concentrate on the formation mechanism of colloidal silica particles. Clearly, when more accurate information about the formation mechanism is obtained, it is possible to control the related parameters. Two models, monomer addition and controlled aggregation, were introduced for the formation mechanism of these particles Matsoukas and Gulari (1988), Bogush and Zukoski (1991), Polte (2015). The monomer addition model describes the achievement of monodisperse silica particles by effective separation of the nucleation and growth processes. It also reveals that the rate of hydrolysis controls the growth of silica particles, and the reaction occurs through the first order reaction in diluted solutions of TEOS. In contrast, the controlled aggregation-based model proposes that uniformly sized particles can be achieved when the aggregation rate between larger particles is slower than that between smaller particles, and growth occurs when the aggregates reach a specific size due to the gathering of small particles. Many studies have been conducted to investigate the reliability of these models and their consistency with the reaction mechanism using different analytical methods, such as DLS, ^{29}Si nuclear magnetic resonance (NMR), ^{13}C NMR, and X-ray scattering Van Blaaderen *et al*. (1992), Kumar *et al*. (2021).

To the best of our knowledge, though computational and modeling analysis have been used in innumerable fields of study Hou *et al*. (2021), Huang *et al*. (2021a, b), Zhao *et al*. (2021), statistical studies investigating the synthesis process of colloidal materials and nanoparticles are limited. Guldin *et al*. (2019) used DOE software to control the mean diameter and dispersity of oleylamine-capped gold nanoparticles (AuNPs) Fhionnlaoich *et al*. (2019). In another study, Khademolhosseini investigated the synergetic effects between silica nanoparticles, bio-surfactant and salinity for increasing the productivity of the oil recovery process Khademolhosseini *et al*. (2019). Despite the daily increase in nanoparticle applications in various fields, only a limited number of published papers have statistically investigated the implementation and synthesis of these invaluable materials Crowson *et al*. (2020), Hiszpanski *et al*. (2020), Altintas *et al*. (2021), Dai *et al*. (2021), Nezadi *et al*. (2021). In this study, the dominant parameters influencing the Stöber method are extracted from the literature Stöber *et*

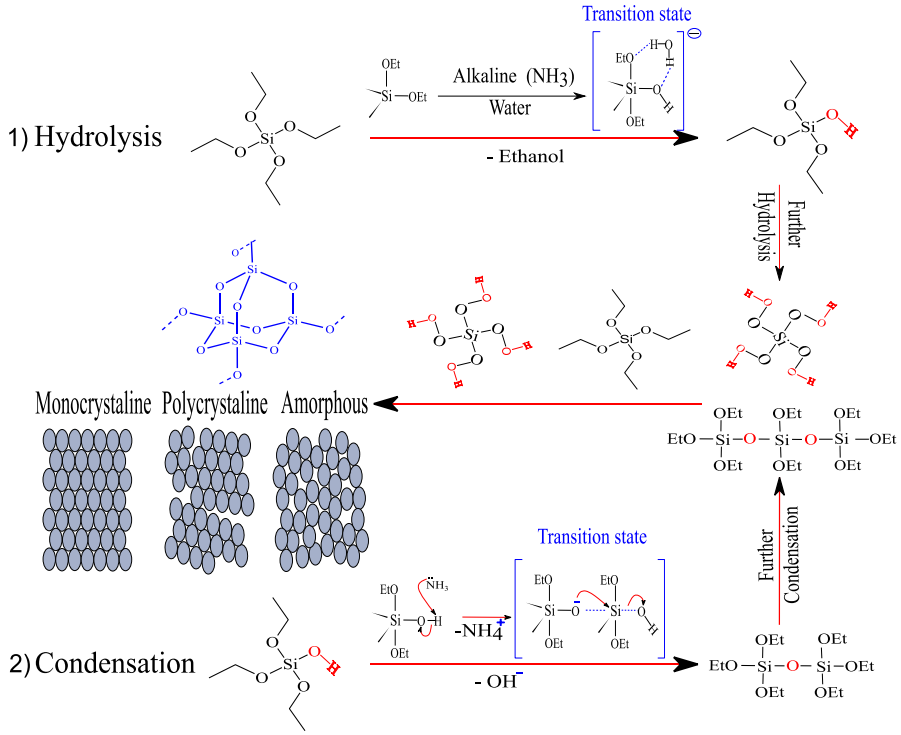

Fig. 2 Hydrolysis and condensation steps in the Stöber method.

Table 3 Studies investigated the Stöber method for synthesis of silica nanoparticles

Investigated Parameters	Method	Reference
pH, Kinetic of hydrolysis reaction	OFAT	Aelion *et al.* (1950)
Formation mechanism and Kinetic of Sol formation	OFAT	LaMer and Dinegar (1950)
NH_3 and TEOS concentration	OFAT	Stöber *et al.* (1968)
Effect other silicate precursors like TMOS, HMOS, OMOS	OFAT	Klemperer *et al.* (1986)
Temperature effect	OFAT	Tan *et al.* (1987)
Temperature and medium effect	OFAT	Tan *et al.* (1987)
TEOS and NH_3 concentration, formation mechanism	OFAT	Matsoukas and Gulari (1988)
Formation mechanism	OFAT	Kim and Zukoski (1990)
TEOS concentration and medium effect	OFAT	Harris *et al.* (1990)
Formation mechanism and kinetics	OFAT	Bogush and Zukoski (1991)
TEOS, H_2O and NH_3 Concentration	OFAT	Bogush and Zukoski (1991)
Effect of TEOS, H_2O, NH_3 concentration, temperature and reaction medium on morphology and chemical microstructure	OFAT	van Blaaderen and Kentgens (1992)
Formation mechanism	OFAT	Bailey and Mecartney (1992)
Particle formation and growth mechanism	OFAT	van Blaaderen *et al.* (1992)
Temperature and TEOS, H_2O, NH_3 concentration effect	OFAT	Giesche (1994)
TEOS, NH_3, H_2O concentration and formation mechanism	OFAT	Lee *et al.* (1997)
Formation mechanism and medium effect	OFAT	Boukari *et al.* (1997)
TEOS, H_2O, NH_3 and formation mechanism	OFAT	Lee *et al.* (1998)
NH_3 and H_2O concentration and medium effects	OFAT	Green *et al.* (2003)
NH_3 concentration	OFAT	Costa *et al.* (2003)
pH effect, microemulsion synthesis	OFAT	Finnie *et al.* (2007)
Formation mechanism	OFAT	Carcouët *et al.* (2014)
NH_3 and LiOH concentration effect and formation mechanism	OFAT	Han *et al.* (2017)
NH_3, TEOS, Temperature effects	CCD/RSM	This study

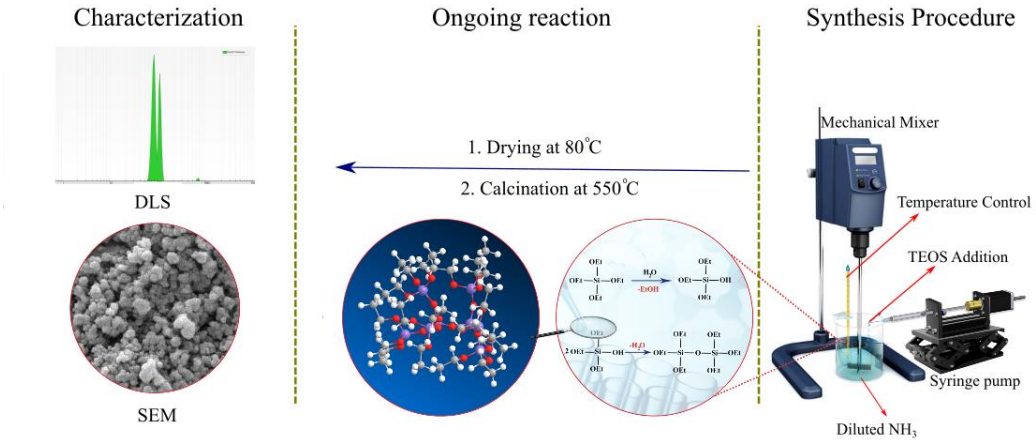

Fig. 3 Graphical abstract of the method to synthesize monodisperse silica

Table 4 Determination of the DOE required parameters and their ranges

Name	*Unit*	*-1 level*	*+1 level*	-α	+α
TEOS	mol/L	0.48	1.31	0.2	1.6
NH_3	mol/L	0.90	2.09	0.5	2.5
Temperature	°C	16.08	33.91	10	40

al. (1968), Liu *et al*. (2011), Fuertes *et al*. (2012), Jiang *et al*. (2017) and Table 3 shows the studies which have been done in the synthesis of silica nanoparticle using Stöber method. In all these studies one factor at a time (OFAT) has been adopted to investigate the effective factors in synthesis of silica particulate.

In this study the TEOS and basic catalyst concentration, as well as the temperature of the reaction, are considered the principal factors influencing the size and monodispersity of the synthesized silica particles. Owing to DOE software, these parameters and central composite design have been used to build a second-order (quadratic) model for the response variables without requiring a complete three-level factorial experiment. Once the experimental results of the trials are obtained and analyzed, two models are suggested by DOE and Python. The accuracy of the suggested models is evaluated by performing a synthesis based on the recommended values for determining factors. Additionally, the optimized reaction conditions to achieve the minimum particle size with the lowest level of TEOS as a valuable reactant are experimentally investigated.

2. Experimental

2.1 Materials and synthesis method

Tetraethyl orthosilicate (ethyl silicate, $Si(OC_2H_5)_4$, 40%) was purchased from Evonik Industries. Ammonia (NH_4OH (aq), 22%) was provided by Razi Petrochemical Industries. Ethanol (EtOH, C_2H_5OH, 99.5%) was obtained from Merck, and distilled water was purchased as a raw material. All reagents used in this study were used directly without further purification.

2.2 Synthesis of monodisperse silica particles

Silica particles were synthesized under basic conditions. For this purpose, according to Table 4 generated by the DOE software after determining the range of concentrations and temperature, the required amount of ammonia solution was poured into a beaker and stirred mechanically at 600 rpm. In order to decrease the agglomeration during synthesis, dissolver blade has been used for mechanical stirring. Diluted TEOS, at room temperature, was added to the stirred beaker with a syringe pump (BT100-1L from LONGER Co.) at a rate of 1 ml/min. The addition of TEOS resulted in an opaque liquid. After the complete addition of TEOS to the gradually emerging opaque liquid, the beaker contents were stirred vigorously at 850 rpm for another 3 h and then washed with ethanol several times to ensure complete removal of the residual reactants. The obtained suspension was dried in an oven for 24 h at 80°C and calcined in a furnace at 550°C for 2 h. Fig. 3 shows a schematic of the procedure.

2.3 Characterization of the synthesized silica nanoparticles

Hydrodynamic particle sizes and size distributions were measured by DLS using Cordouan technologies at ambient temperature. Each sample was measured three times for better accuracy in reporting the particle size and avoiding reporting agglomerations and sedimentation. The morphology of the silica particles was investigated using scanning electron microscopy (SEM, Philips XL30).

2.4 Statistical approach using DOE

The statistical results of the experiment were obtained using Design Expert V.7.0 statistical software. The morphology and particle size of the colloidal silica particles can be affected by different parameters, such as temperature, TEOS, and catalyst concentration. According to previous studies, the critical concentrations of TEOS and NH_3 that can influence the main properties have been reported as between (0.2–1.6 mol/L) and (0.5–2.5 mol/L), respectively. In addition, the critical temperature was

Table 5 Experimental design

Standard	Run	TEOS mol/L	NH_3 mol/L	Temp °C	Particle size (nm)
7	1	0.48	2.09	33.92	884.6
6	2	1.32	0.91	33.92	96.48
15	3	0.90	1.5	25	108.18
17	4	0.90	1.5	25	271.33
2	5	1.32	0.91	16.08	133.85
3	6	0.48	2.09	16.08	557
18	7	0.90	1.5	25	284.46
10	8	1.60	1.5	25	451.46
4	9	1.32	2.09	16.08	468
8	10	1.32	2.09	33.92	418.7
5	11	0.48	0.91	33.92	81.59
12	12	0.90	2.5	25	458
13	13	0.90	1.5	10	67.81
16	14	0.90	1.5	25	308.02
1	15	0.48	0.91	16.08	98.17
11	16	0.90	0.5	25	158
9	17	0.20	1.5	25	568.88
14	18	0.90	1.5	40	411.58

Table 6 ANOVA results

Source	*Sum of squares*	*DF*	*Mean square*	*F-value*	*P-value*
Model	737 600	8	92 197.60	9.77	0.0021
A-[TEOS]	36 064.81	1	36 064.81	3.82	0.0863
B-[NH_3]	461 400	1	461 400	48.89	0.0001
C-Temperature	47 156.26	1	47 156.26	5.00	0.0558
AB	45 824.24	1	45 824.24	4.86	0.0587
AC	19 769.67	1	19 769.67	2.09	0.1858
BC	13 798.76	1	13 798.76	1.46	0.2611
A^2	137 900	1	137 900	14.61	0.0051
B^2	10 593.51	1	10 593.51	1.12	0.3203
R^2	0.9071				

between 10°C and 40°C (Bogush *et al.* 1988). To achieve the most accurate results and increase the reliability of the software prediction, the aforementioned parameters were chosen in their critical range to design the experiment of the process. For this reason, the beginning (-α) and end (+α) of the variable ranges were defined for the software, and the software generated a low value (-1) and high value (+1). The upper and lower limits of the determining variables are listed in Table 4.

The number of runs in the central composite design model in the DOE software is calculated using the following equation:

$$\text{Number of runs in CCD model: } 2^K + 2K + C \qquad (1)$$

where K is the number of variables and C is the number of central points. (2^K) is defined as the number of factorial

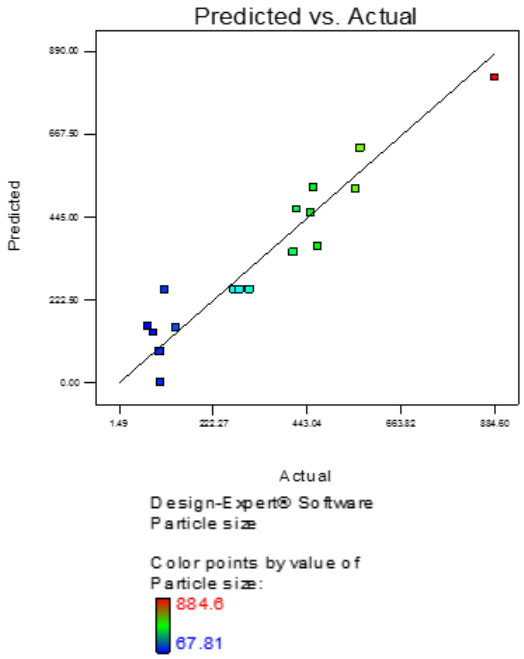

Fig. 4 Comparison between actual and predicted values

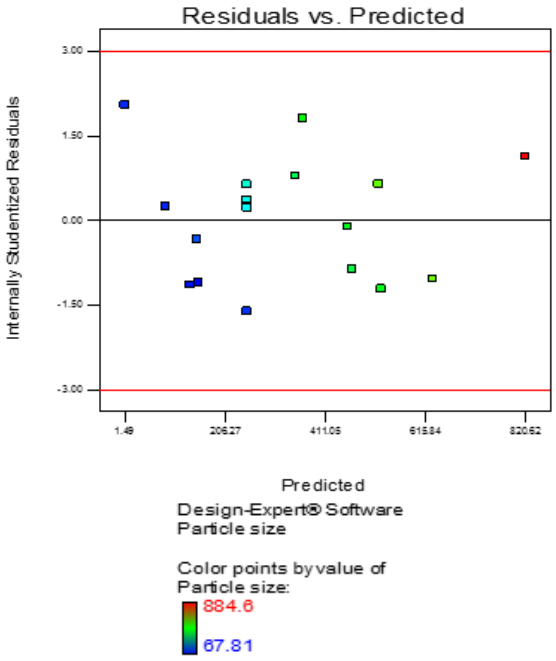

Fig. 5 Deviation of results from the predicted line

tests determined between the range of +1 and -1 levels, and ($2K$) is defined as the number of axial tests in which one variable is between -α and +α and the other variables are located at the central points. According to this definition, the number of experiments required for investigating the Stöber process with three variables (K = 3) and four central points (C = 4) is 18. Table 4 shows the suggested conditions for each run and their observed results. The particle size measured for all the experiments was analyzed by DLS and reported in number.

Table 5 shows the analysis of variance (ANOVA) table acquired after modifying the quadratic model by eliminating

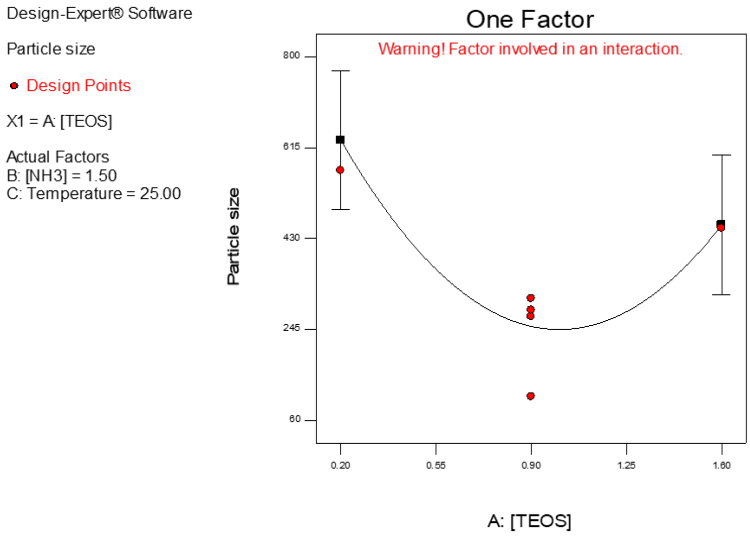

Fig. 6 One-factor approach on the correlation between [TEOS] and particle size ([NH_3] = 1.5 M, temperature = 25°C)

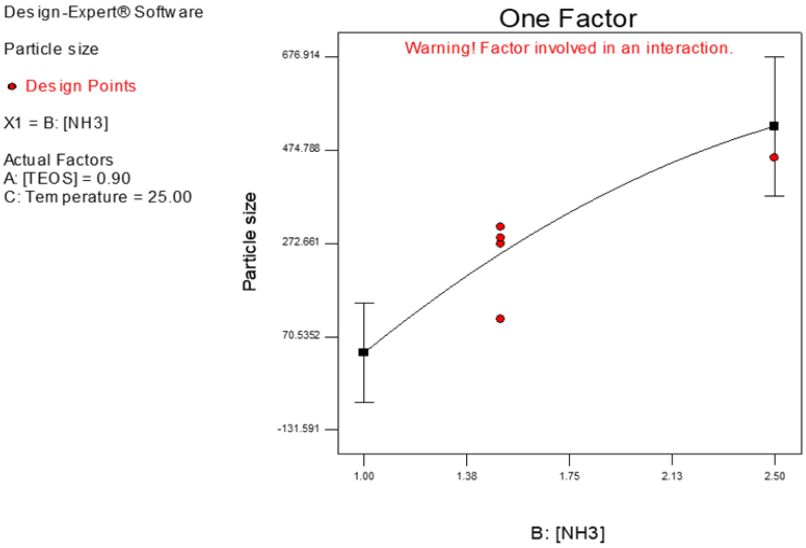

Fig. 7 One-factor approach on the correlation between [NH_3] and particle size ([TEOS] = 0.9 M, temperature = 25°C)

the C^2 intercept. The relatively high R^2 (0.9071) reveals the consistency of the given model with our experimental values. The p-value (0.0021) implies that the model is significant at the 95% confidence level and reliable enough to predict and optimize the reaction conditions. The table also indicates that the concentration of NH_3 with the lowest p-value can be considered the most influential factor on the size of the particles.

After this step, the actual values and predicted values were compared. The high value of R2 corroborated the reliability of the model. As a result, a sensible connection between the actual and predicted values was obtained, and no outlier points were observed. Figs. 4 and 5 are considered evidence to substantiate this assertion.

3. Result and discussion

Since the introduction of five significant parameters that play an essential role in the size of the silica particles by Bogush and Zukoski (1991), many studies have been conducted to investigate the effect of these parameters Rao *et al*. (2005), Rahman *et al*. (2007), all of which have concentrated on the effect of the parameters using the one-factor approach. However, it is obvious that investigation of the parameters with a two-dimensional or even a three-dimensional approach can give rise to more accurate data because not only does this feature help us to determine the correlation between one parameter and the particle size, but it also provides insight into the effects of different parameters on each other Liu *et al*. (2021), Xu *et al*. (2021), Yu *et al*. (2022).

3.1 One-factor approach on variables influencing the particle size of colloidal silica

3.1.1 Effect of TEOS concentration on particle size

Different reports have been published regarding the effect of TEOS concentration on the size of silica nano-

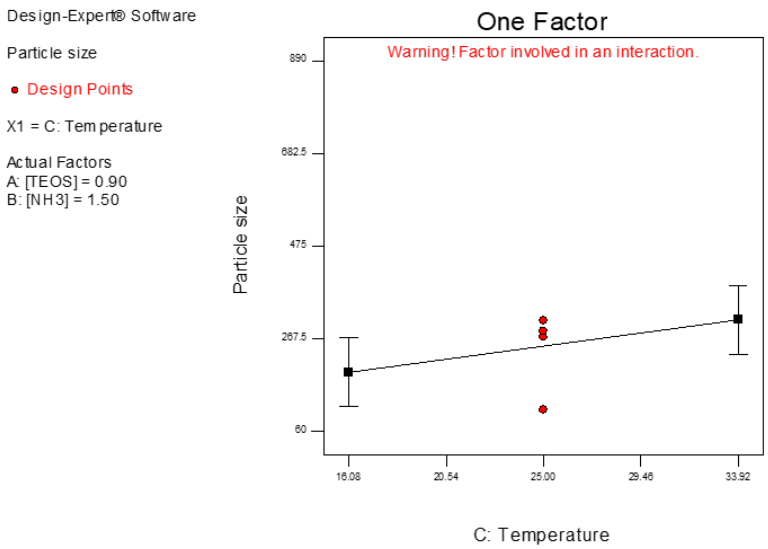

Fig. 8 One-factor approach on the correlation between temperature and particle size at constant concentrations of [TEOS] and [NH_3]

particles. In 1968, Stöber *et al*. (1968) found no connection between TEOS concentration and particle size. After nearly two decades, van Helden found an indirect relationship and reported a reduction in particle size by increasing the TEOS concentration Van Helden *et al*. (1981), and seven years later, Bogush *et al*. (1988) published an article implying that when the concentration of TEOS was increased, the particle size increased. Despite some clear discrepancies between the reports, all the results are sufficiently accurate and the only difference between them is the lack of simultaneous study of the effects of other parameters on the concentration of TEOS.

In the present study, it was revealed that increasing the TEOS concentration in the range of ($0.2 < M < 1.1$) at (1.5 M) NH_3 and ambient temperature (25°C) led to a reduction in particle size; nevertheless, a further increase in concentration of TEOS ($M > 1$ mol/L) reversed this trend and resulted in a steep increase in particle size (Fig. 6). The observed turning point in the TEOS concentration effect may be due to a longer induction time in dilute solutions of TEOS. Nucleation occurs when the concentration of monomers reaches a critical supersaturation level. After that, primary particles appear, and if their concentration increases to the level of C_{min} (The minimum concentration required to ignite the aggregation of the primary particles), they may aggregate to form stable secondary particles. Nucleation continues and more nuclei are formed when the concentration of monomers in the reaction system is reduced below the nucleation threshold. Subsequently, if the concentration of the catalyst is sufficient and the temperature of the reaction is able to provide sufficient energy for effective collisions, an acceleration occurs in condensation reactions between two silicic acid monomers, causing monomer addition on the surfaces of the primary particles LaMer and Dinegar (1950), Svirbely and Mador (1950). As shown in Fig. 6, increasing the concentration of TEOS raises the possibility of reaching the supersaturation point specifically when ([TEOS] > 1 mol/L). In this situation, when the reaction conditions can provide enough energy to pass the activation barrier, the rate of condensation reaction increases, and growth can overcome nucleation. Hence, larger particles were observed.

3.1.2 Effect of NH_3 concentration on particle size

Increasing the concentration of ammonia leads to larger particles by increasing the rate of hydrolysis and condensation in the formation mechanism of silica. As a result, a lower concentration of the base catalyst facilitates smaller particles Matsoukas and Gulari (1988), Rahman *et al*. (2007). Fig. 7 substantiates this assertion by showing the relation between [NH_3] and particle size of the synthesized silica.

3.1.3 Effect of reaction temperature on particle size

According to the literature, the correlation between temperature and particle size is indirect. Research based on the monomer addition model highlights a decrease in the rate of hydrolysis reactions with decreasing temperature, so it seems rational that a much smaller number of particles appears to relieve the high supersaturation of silicic acid (C_{sat} = the maximum possible quantity of a substance that can dissolve in a standard volume of a specific solvent). As a result, for a fixed amount of TEOS in each reaction, the average particle size must increase as the temperature is reduced. However, we found that the relationship between temperature and particle size is slightly more complex than the effects of other parameters because the temperature can influence the solubility of the base catalyst and silica sources and impact the viscosity of the solution. Essentially, in the one-factor approach, as shown in Fig. 8, when the temperature is increased, the particle size increases slightly at constant concentrations of [TEOS] = 0.9 and [NH_3] = 1.5, yet the trend can be totally different at other concentrations. Clearing the relationship between the reaction temperature and particle size, the temperature effect is discussed in two-dimensional approaches.

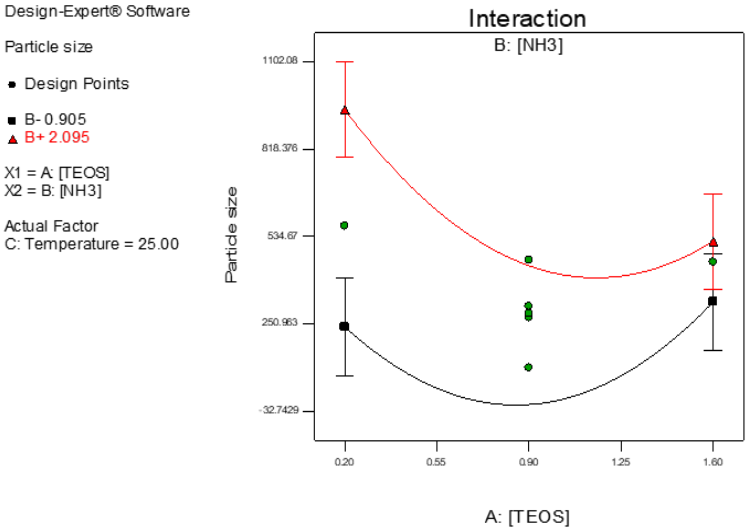

Fig. 9 Interaction between [TEOS] and [NH_3] at ambient temperature

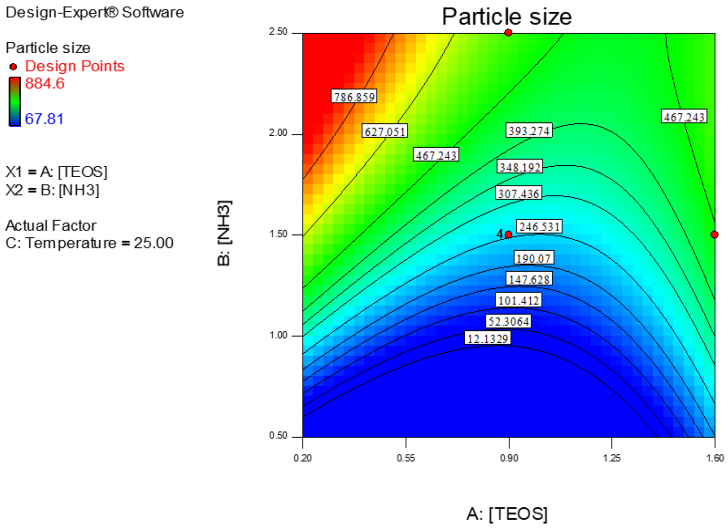

Fig. 10 Contour lines of [TEOS] and [NH_3] as variables at ambient temperature

3.2 Two-factor approach on variables influencing the particle size of colloidal silica

3.2.1 Simultaneous change of [TEOS] and [NH_3] variables at constant temperature

As mentioned above, the one-factor investigation graph does not appear sufficiently complete to analyze a process Oyarhossein *et al*. (2020), Al-Furjan *et al*. (2021), Hou *et al*. (2021). Despite a clear trend in Figs. 6-8, these graphs are only reliable for specific concentrations and temperatures, and the trend can be varied by changing these parameters. Consequently, the contour lines of a function with two variables and interaction graphs are prioritized for a better analysis. Fig. 9 illustrates the relationship between [TEOS] and [NH_3] at 25°C. This graph is considered a two-dimensional factor, which is known as an interaction graph. In this type of investigation, one variable (temperature) remains constant, and the two other variables ([TEOS], [NH_3]) change simultaneously Huo *et al*. (2021), Peng *et al*. (2021). The graph shows that the interaction between the TEOS concentration and ammonia solution is relatively conceivable at higher concentrations. As a result, at constant concentrations of TEOS, an increase in the concentration of NH_3 contributes to larger particles.

The same trend can be seen more explicitly in Fig. 10, where the contour lines show the variation of [TEOS] with [NH_3] and their simultaneous effect on particle size. Clearly, increasing the concentration of ammonia at a specific concentration of TEOS increases the particle size and the curves move from the blue region (smaller particles) to the green and yellow regions (larger particles).

3.2.2 Simultaneous change of [TEOS] and temperature variables at constant concentration of ammonia

The effects of [TEOS] and temperature on each other and their impact on particle size appear considerable. As shown in Fig. 11, the interaction between the concentration

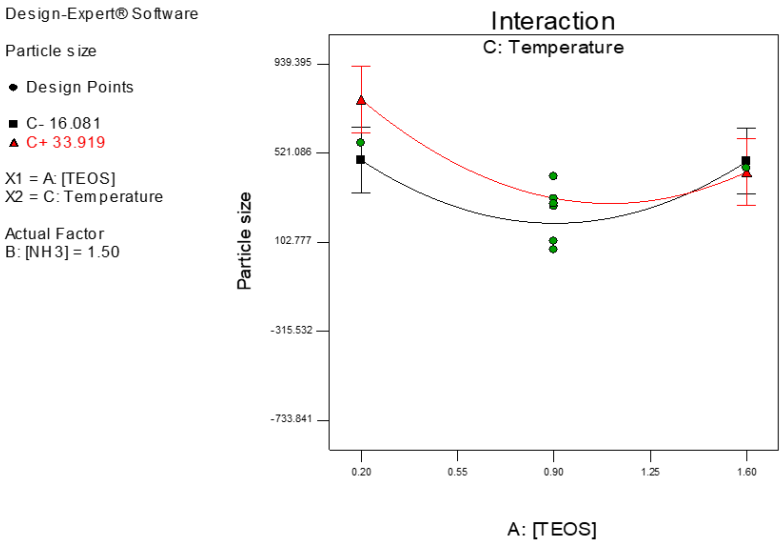

Fig. 11 Interaction between [TEOS] and temperature at constant concentration of base catalyst

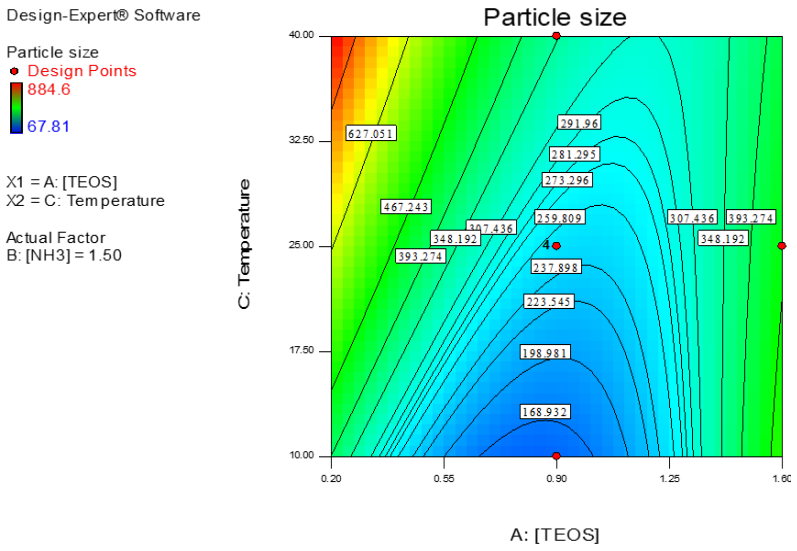

Fig. 12 Contour lines of [TEOS] and temperature as variables at constant concentration of ammonia

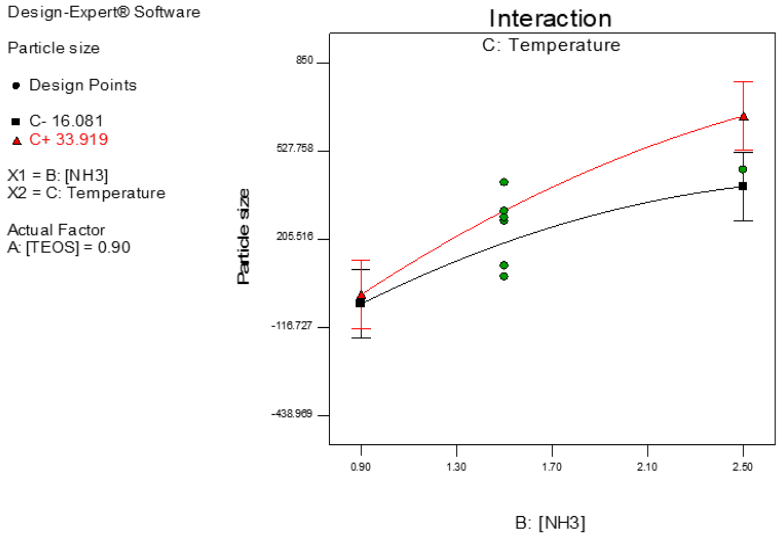

Fig. 13 Contour lines of [TEOS] and temperature as variables at constant concentration of ammonia

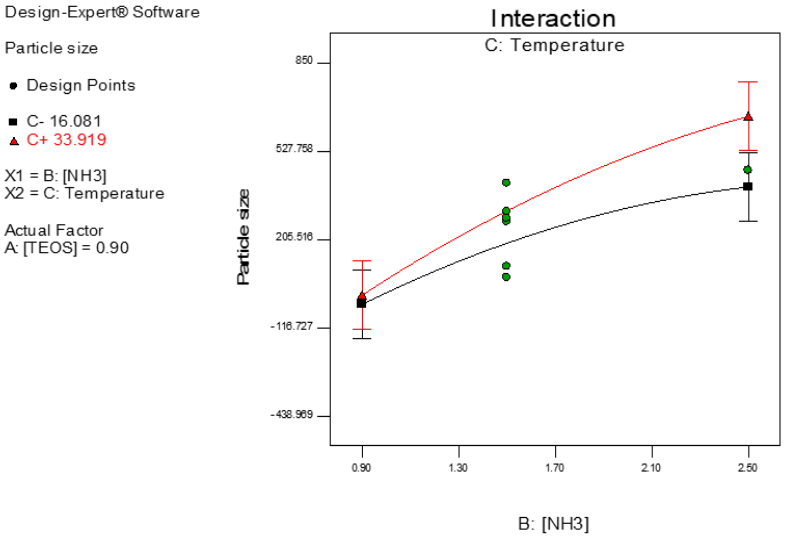

Fig. 14 Interaction between [NH_3] and temperature at constant concentration of TEOS

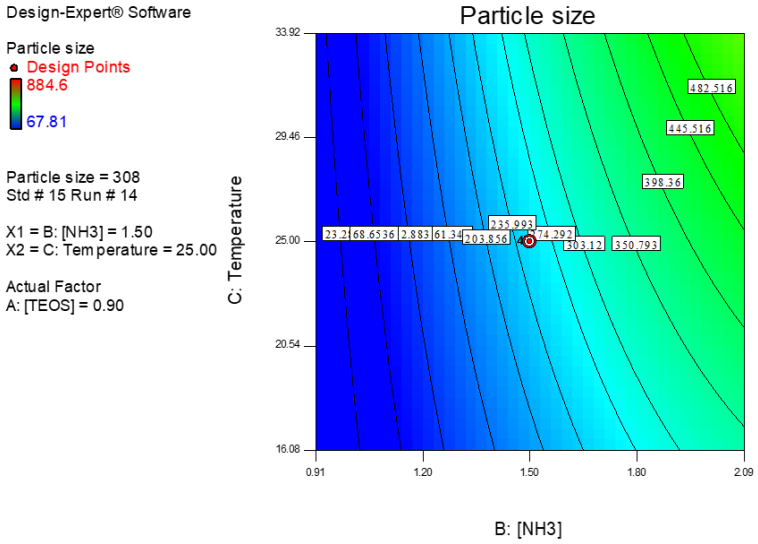

Fig. 15 Contour lines of [NH_3] and temperature as variables at constant concentration of [TEOS]

of TEOS and temperature is intense, specifically at higher concentrations when [TEOS] > 1.3 M. In other words, at a constant concentration of the base catalyst [NH_3] = 1.5, increasing the concentration of TEOS to 1.3 contributes to a smaller particle size; however, after this critical point, the particle size increases. As stated in Section 3.1.3, the effect of temperature is more complicated because this parameter can alter multiple factors simultaneously, such as viscosity and solubility, and provide sufficient energy to pass the activation energy and control the nucleation and growth steps in the formation of particles. Consequently, further experiments and investigations are required to elucidate the kinetics and mechanism of the formation reactions.

A more explicit trend can be seen in Fig. 12, where the contour lines depict the particle size changes at various temperatures. More obvious is the fact that at a given temperature and constant concentration of ammonia, byincreasing the concentration of TEOS, the particle size decreases, and then at higher concentrations of TEOS [*M* > 1.1 mol/L], the trend is reversed, and the particle size increases. In fact, by moving horizontally on the graph, we enter the blue region (smaller particles) from the green region (bigger particles) and then enter the green region again by moving forward.

3.2.3 Simultaneous change of [NH_3] and temperature variables at a constant concentration of TEOS

Our study reveals a synergistic effect between the concentration of the base catalyst and temperature on the particle size. This effect is even more considerable at higher concentrations of the base catalyst and elevated temperatures. As shown in Fig. 13, the slope of the graphs is steeper and changes more at higher temperatures, indicating the effect of temperature on larger particle sizes. More accurate investigations can be carried out by interpreting Fig. 14, where the interaction of [NH_3] and temperature is depicted more tangibly. The contour graphs in Fig. 15 indicate that at certain concentrations of ammonia and a constant

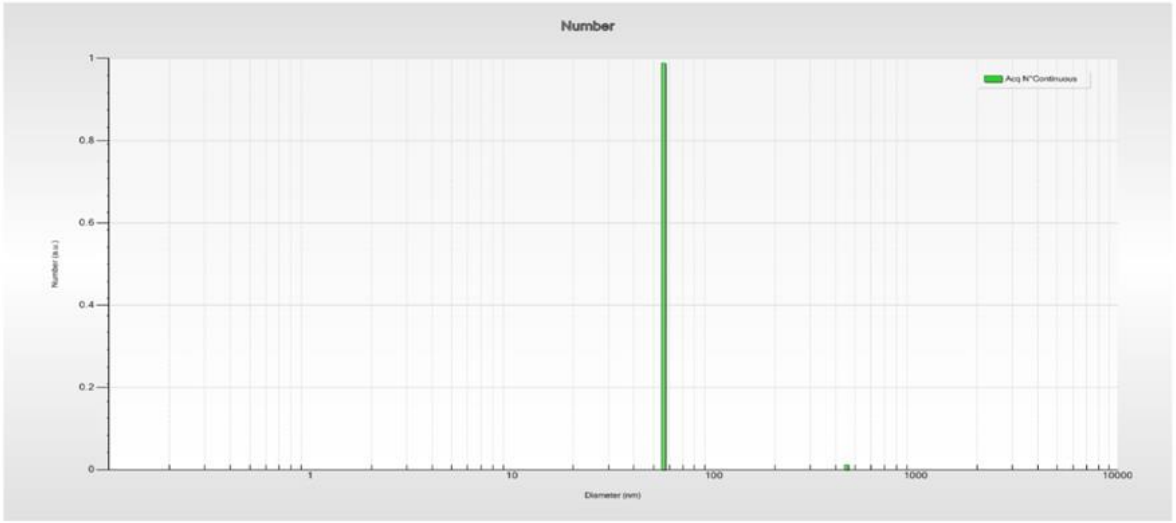

Fig. 16 DLS analysis of the optimized silica nanoparticles.

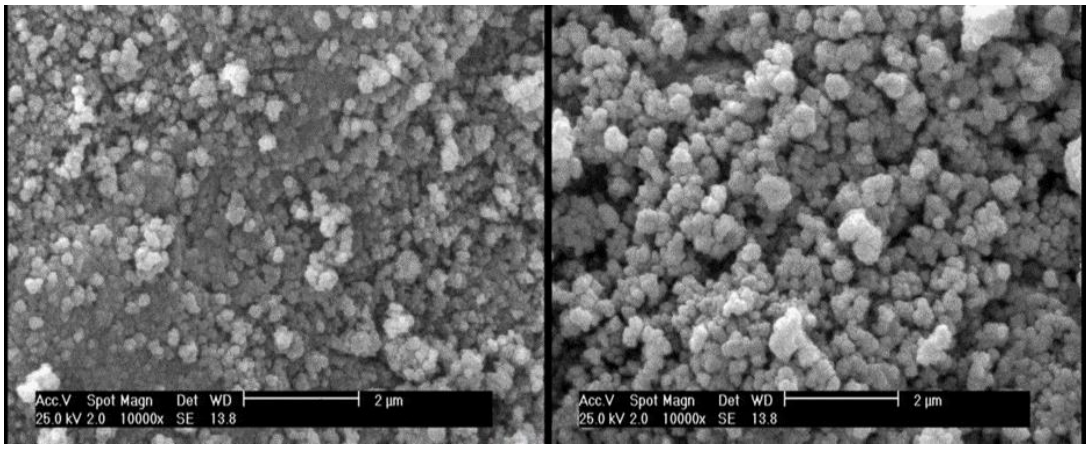

Fig. 17 SEM analysis of the silica nanoparticles

concentration of TEOS, increasing the temperature leads to slow growth of the particle size, and as the concentration of [NH_3] increases, the trend of increasing particle size accelerates.

3.3 Optimizing the reaction conditions

The central composite design (CCD) method was used to optimize the reaction conditions to obtain the minimum particle size while considering minimal TEOS consumption. As a result, variables were optimized using statistical tools, and experimental tests were carried out for confirmation. TEOS can be considered a more expensive reactant in comparison with other chemicals, and consequently, the lower the concentration, the more economical the industrial production of nanosilica. According to the statistical calculation of the CCD method, the most optimum condition for obtaining particles below 100 nm is [TEOS] = 0.48 mol/L, [NH_3] = 0.91 mol/L, and a temperature of 33.37°C. The accurate prediction of the CCD method was 67 nm, which was approximately consistent with the DLS analysis (56.36 nm) of the particles synthesized in the laboratory (Fig. 16). SEM analysis was also conducted to investigate the morphology of the synthesized silica (Fig. 17).

4. Machine-learning prediction

In recent years, artificial intelligence has become a powerful tool in many scientific research areas Qiao *et al.* (2021), Xu *et al*. (2021), Ma *et al*. (2021b). It is seen that

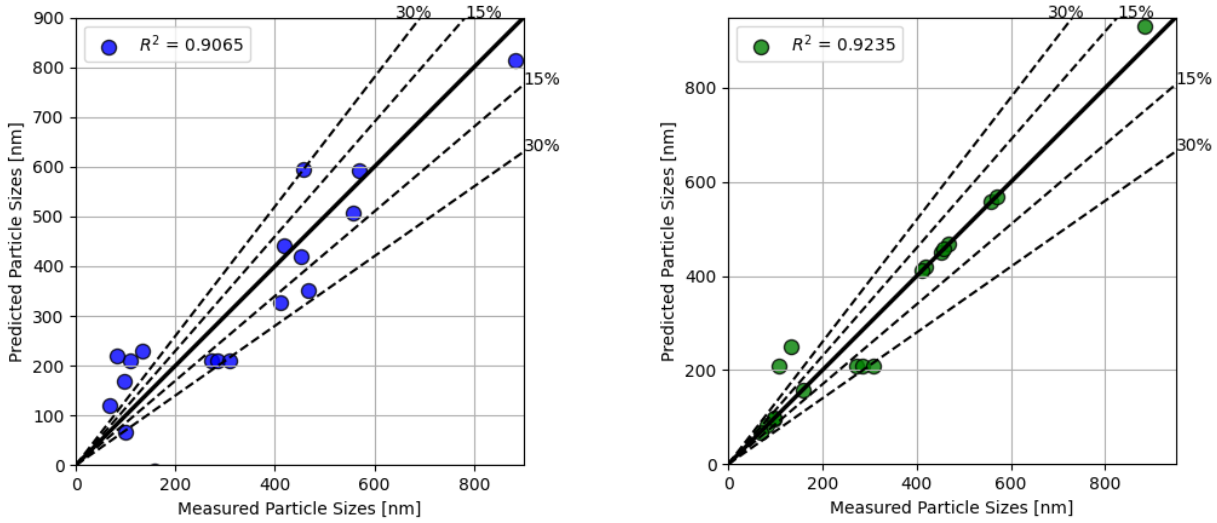

(a) Quadratic polynomial regression models (b) Third-order polynomial regression models

Fig. 18 Comparison of the predicted particle size using a machine-learning model for quadratic and third-order polynomial regression models and actual measured sizes of particles. The black line represents $x = y$

experimental and numerical simulations of many physical problems require time consuming practices (Amelirad and Assempour 2019, 2021, Zhou *et al.* 2020, Al-Furjan *et al.* 2021, Dai *et al.* 2021a, b, c, d, Ebrahimi *et al.* 2021, Ghabussi *et al.* 2021, Guo *et al.* 2021a, b, Hashemi *et al.* 2021, He *et al.* 2021, Huang *et al.* 2021c, Huo *et al.* 2021, Liu *et al.* 2021a, b, Moayedi *et al.* 2021, Najaafi *et al.* 2021, Peng *et al.* 2021, Shao *et al.* 2021, Shariati *et al.* 2021, Wu and Habibi 2021, Zhang *et al.* 2021a, b, c) Thus, machine learning capability in predicting new results based on previous experiments and datasets with extraordinarily low computational cost (He *et al.* 2020, Li *et al.* 2020), in addition to providing practically exact results, has attracted the attention of many researchers (Jinnouchi and Asahi 2017, Cao *et al.* 2018, Yang *et al.* 2019, Acar 2020, Altintas *et al.* 2021). In the present study, this method was also applied to the original dataset to construct a prediction model using quadratic and third-order regression polynomials Li *et al.* (2020). The Scikit-learn package (Abraham *et al.* 2014, Wang *et al.* 2020) in Python was chosen to create the machine model using the data given in Table 4. The input data were the set of TEOS, NH_3, and temperature, and the output data were the particle sizes. To create a polynomial model, many trials were conducted to find the best selection of data to train the model. Accordingly, it was found that selection of 80% of the dataset for training the model presented the best outcome. Furthermore, the code was run several times to find the best scored model in terms of mean squared error. Finally, the predicted results were compared with the actual particle sizes, as shown in Fig. 18. The selected models have $R^2 = 0.9065$ for the quadratic model and $R^2 = 0.9235$ for the third-order model, which can be regarded as a virtuous score for the model based on the selected test and training sets of data.

The calculated machine-learning model was further saved and employed for the prediction of the resultant particle size for $[\mathrm{TEOS}] = 0.48\ \mathrm{mol/L}$, $[\mathrm{NH_3}] = 0.91\ \mathrm{mol/L}$ and temperature $T = 33.37\ ^{\circ}\mathrm{C}$ as given in section 3.3. For this single dataset the predicted particle size was $\mathrm{PS} = 215.35\ \mathrm{nm}$ in the quadratic model and $\mathrm{PS} = 81.59\ \mathrm{nm}$ in the third-order model. The quadratic model result was far from the actual measured particle size of $56.36\ \mathrm{nm}$ but the third-order model presented a more reasonable outcome.

The training procedure of a machine model usually requires a larger set of data to predict more accurate results. However, with the data available in the present study, the predicted values are acceptable in terms of the computational cost and effort required to obtain the results. Nevertheless, this method still provides high computational efficiency in comparison to other analytical and mathematical methods (Alipour *et al.* 2020, Cheshmeh *et al.* 2020, Li *et al.* 2020, Liu *et al.* 2020, Moayedi *et al.* 2020a, b, Shariati *et al.* 2020, Shi *et al.* 2020).

5. Conclusions

Silica nanoparticles were synthesized by the Stöber method using TEOS as an initiator and simultaneously investigating three main parameters: TEOS concentration, NH_3 concentration, and temperature. The CCD model, suggested by DOE software, was used to build a quadratic model. Achieving minimum particle size with the lowest possible consumption of TEOS was considered the main goal of the designed experiments. The results revealed that a one-factor investigation is not a reliable approach to evaluate the effects of different parameters on the size of the nanoparticles, and these results can only be satisfactory for specific temperatures and concentrations. On the other hand, the size of nanoparticles synthesized under optimized conditions, as suggested by the DOE software model, ascertained that evaluation based on the results of two variables concurrently and consideration of their interaction

can give rise to more valid results. Comparing the quadratic models generated by the DOE and the Scikit-learn package in Python with the third-order model, it was found that the third-order model is more satisfactory for assessment of the simulated and actual results. Since all the materials used in this study were industrial grades, the results of this study can be applicable in laboratory and semi-industrial synthesis of nanosilica particles with a defined range of size. Moreover, the statistical method represented in this study, will be a promising approach to tackle the time and cost of trials required for synthesis of the silica nanoparticles with the desired size and abundance.

Acknowledgment

The authors are very grateful to the Korea Environment Industry & Technology Institute (research grant number: 2020002470002), Republic of Korea. The work reported in this paper was conducted during the sabbatical year of Kwangwoon University in 2021.

References

Abraham, A., Pedregosa, F., Eickenberg, M., Gervais, P., Mueller, A., Kossaifi, J., Gramfort, A., Thirion, B. and Varoquaux, G. (2014), "Machine learning for neuroimaging with scikit-learn", *Front. Neuroinform.*, **8**, 14. https://doi.org/10.3389/fninf.2014.00014.

Abulateefeh, S.R., Spain, S.G., Aylott, J.W., Chan, W.C., Garnett, M.C. and Alexander, C. (2011), "Thermoresponsive polymer colloids for drug delivery and cancer therapy", *Macromol. Biosci.*, **11**(12), 1722-1734. https://doi.org/10.1002/mabi.201100252.

Acar, P. (2020), "Machine learning reinforced crystal plasticity modeling under experimental uncertainty", *AIAA J.*, **58**(8), 3569-3576. https://doi.org/10.2514/1.J059233

Aelion, R., Loebel, A. and Eirich, F. (1950), "Hydrolysis of Ethyl Silicate*", *J. Am. Chem. Soc.*, **72**(12), 5705-5712. https://doi.org/10.1021/ja01168a090.

Al-Furjan, M.S.H., Dehini, R., Khorami, M., Habibi, M. and won Jung, D. (2021), "On the dynamics of the ultra-fast rotating cantilever orthotropic piezoelectric nanodisk based on nonlocal strain gradient theory", *Compos. Struct.*, **255**, 112990. https://doi.org/10.1016/j.compstruct.2020.112990.

Alipour, M., Torabi, M.A., Sareban, M., Lashini, H., Sadeghi, E., Fazaeli, A., Habibi, M. and Hashemi, R. (2020), "Finite element and experimental method for analyzing the effects of martensite morphologies on the formability of DP steels", *Mech. Based Des. Struct.*, **48**(5), 525-541. https://doi.org/10.1080/15397734.2019.1633343.

Altintas, C., Altundal, O.F., Keskin, S. and Yildirim, R. (2021), "Machine Learning Meets with Metal Organic Frameworks for Gas Storage and Separation", *J. Chem. Inf. Model.*, **61**(5), 2131-2146. https://doi.org/10.1021/acs.jcim.1c00191.

Amelirad, O. and Assempour, A. (2019), "Experimental and crystal plasticity evaluation of grain size effect on formability of austenitic stainless steel sheets", *J. Manuf. Proc.*, **47**, 310-323. https://doi.org/10.1016/j.jmapro.2019.09.035.

Amelirad, O. and Assempour, A. (2021), "Coupled continuum damage mechanics and crystal plasticity model and its application in damage evolution in polycrystalline aggregates", *Eng. Comput.*, 1-15. https://doi.org/10.1007/s00366-021-01346-2.

Arani, A.G., Farazin, A. and Mohammadimehr, M. (2021), "The effect of nanoparticles on enhancement of the specific mechanical properties of the composite structures: A review research", *Adv. Nano Res.* **10**(4), 327-337. https://doi.org/10.12989/ANR.2021.10.4.327.

Bai, B., Nie, Q., Zhang, Y., Wang, X. and Hu, W. (2021), "Cotransport of heavy metals and SiO_2 particles at different temperatures by seepage", *J. Hydrol.*, **597**, 125771. https://doi.org/10.1016/j.jhydrol.2020.125771.

Bai, Y., Alzahrani, B., Baharom, S. and Habibi, M. (2020), "Semi-numerical simulation for vibrational responses of the viscoelastic imperfect annular system with honeycomb core under residual pressure", *Eng. Comput.*, 1-26. https://doi.org/10.1007/s00366-020-01191-9.

Bailey, J.K. and Mecartney, M.L. (1992), "Formation of colloidal silica particles from alkoxides", *Colloid Surf.*, **63**(1), 151-161. https://doi.org/10.1016/0166-6622(92)80081-C.

Bergna, H.E. (2005), "The language of colloid science and silica chemistry", *Colloid. Silica.*, 5-7. https://doi.org/10.1201/9781420028706-6.

Bogush, G.H. and Zukoski, C.F. (1991), "Studies of the kinetics of the precipitation of uniform silica particles through the hydrolysis and condensation of silicon alkoxides", *J. Colloid Interf. Sci.*, **142**(1), 1-18. https://doi.org/10.1016/0021-9797(91)90029-8.

Boukari, H., Lin, J.S. and Harris, M.T. (1997), "Probing the dynamics of the silica nanostructure formation and growth by SAXS", *Chem. Mater.*, **9**(11), 2376-2384. https://doi.org/10.1021/cm9702878.

Cao, B., Adutwum, L.A., Oliynyk, A.O., Luber, E.J., Olsen, B.C., Mar, A. and Buriak, J.M. (2018), "How to optimize materials and devices via design of experiments and machine learning: Demonstration using organic photovoltaics", *ACS Nano*, **12**(8), 7434-7444. https://doi.org/10.1021/acsnano.8b04726.

Carcouët, C.C., van de Put, M.W., Mezari, B., Magusin, P.C., Laven, J., Bomans, P.H., Friedrich, H., Esteves, A.C., Sommerdijk, N.A., van Benthem, R.A. and de With, G. (2014), "Nucleation and growth of monodisperse silica nanoparticles", *Nano Lett.*, **14**(3), 1433-1438. https://doi.org/10.1021/nl404550d.

Cerbelaud, M., Videcoq, A., Rossignol, F., Piechowiak, M.A., Bochicchio, D. and Ferrando, R. (2016), "Heteroaggregation of ceramic colloids in suspensions", *Adv. Physi X*, **2**(1), 35-53. https://doi.org/10.1080/23746149.2016.1254064.

Cheshmeh, E., Karbon, M., Eyvazian, A., Jung, D.W., Habibi, M. and Safarpour, M. (2020), "Buckling and vibration analysis of FG-CNTRC plate subjected to thermo-mechanical load based on higher order shear deformation theory", *Mech. Based Des. Struct.*, 1-24. https://doi.org/10.1080/15397734.2020.1744005.

Costa, C.A.R., Leite, C.A.P. and Galembeck, F. (2003), "Size dependence of Stöber silica nanoparticle microchemistry", *J. Phys. Chem. B*, **107**(20), 4747-4755. https://doi.org/10.1021/jp027525t.

Crowson, M.G., Lin, V., Chen, J.M. and Chan, T.C.Y. (2020), "Machine learning and cochlear implantation-a structured review of opportunities and challenges", *Otol. Neurotol.*, **41**(1), e36-e45. https://doi.org/10.1097/MAO.0000000000002440.

Curley, R., Holmes, J.D. and Flynn, E.J. (2021), "Can sustainable, monodisperse, spherical silica be produced from biomolecules? A review", *Appl. Nanosci.*, **11**(6), 1777-1804. https://doi.org/10.1007/s13204-021-01869-6.

Dai, Z., Jiang, Z., Zhang, L. and Habibi, M. (2021a), "Frequency characteristics and sensitivity analysis of a size-dependent laminated nanoshell", *Adv. Nano. Res.*, **10**(2), 175-175. https://doi.org/10.12989/ANR.2021.10.2.175.

Dai, Z., Zhang, L., Bolandi, S.Y. and Habibi, M. (2021b), "On the vibrations of the non-polynomial viscoelastic composite open-

type shell under residual stresses", *Compos. Struct.*, **263**, 113599. https://doi.org/10.1016/j.compstruct.2021.113599.

Dai, Z.C., Jiang, Z.Y., Zhang, L. and Habibi, M. (2021c), "Frequency characteristics and sensitivity analysis of a size-dependent laminated nanoshell", *Adv Nano Res.* **10**(2), 175-189. https://doi.org/10.12989/anr.2021.10.2.175.

de Moraes, A.C.P., Ribeiro, L.D.S., de Camargo, E.R. and Lacava, P.T. (2021), "The potential of nanomaterials associated with plant growth-promoting bacteria in agriculture", *3 Biotech.*, **11**(7), 318. https://doi.org/10.1007/s13205-021-02870-0.

Dickinson, E. (2015), "Colloids in food: Ingredients, structure, and stability", *Ann. Rev. Food Sci. Technol.*, **6**, 211-233. https://doi.org/10.1146/annurev-food-022814-015651.

Ebrahimi, F., Mohammadi, K., Barouti, M.M. and Habibi, M. (2021), "Wave propagation analysis of a spinning porous graphene nanoplatelet-reinforced nanoshell", *Wave. Random Complex Med.*, **31**(6), 1655-1681. https://doi.org/10.1080/17455030.2019.1694729.

Everett, D.H. (1972), "Manual of Symbols and Terminology for Physicochemical quantities and units, appendix II: Definitions, terminology and symbols in colloid and surface chemistry", *Pure Appl. Chem.*, **31**(4), 577-638. https://doi.org/10.1351/pac197231040577.

Feng, T., Liu, N., Wang, S.J., Qin, C., Shi, S.W., Zeng, X.Y. and Liu, G. (2021), "Research on the dispersion of carbon nanotubes and their application in solution-processed polymeric matrix composites: A review", *Adv. Nano. Res.*, **10**(6), 559-576. https://doi.org/10.12989/anr.2021.10.6.559.

Fhionnlaoich, N.M., Yang, Y., Qi, R., Galvanin, F. and Guldin, S. (2019), "DoE-It-Yourself: A case study for implementing design of experiments into nanoparticle synthesis", *Chem. Eng. Ind. Chem.*, 2019. https://doi.org/10.26434/chemrxiv.8198420.v1.

Finnie, K.S., Bartlett, J.R., Barbé, C.J. and Kong, L. (2007), "Formation of silica nanoparticles in microemulsions", *Langmuir*, **23**(6), 3017-3024. https://doi.org/10.1021/la0624283.

Fu, H., Gao, B., Hu, C., Liu, Z., Hu, L., Kan, J., Feng, Z. and Xing, P. (2021), "3D nitrogen-doped graphene created by the secondary intercalation of ethanol with enhanced specific capacity", *Nanotechnology*, **33**(7). https://doi.org/10.1088/1361-6528/ac30c2.

Fuertes, A.B., Valle-Vigon, P. and Sevilla, M. (2012), "One-step synthesis of silica@resorcinol-formaldehyde spheres and their application for the fabrication of polymer and carbon capsules", *Chem. Commun.*, **48**(49), 6124-6126. https://doi.org/10.1039/c2cc32552g.

Ghabussi, A., Habibi, M., NoormohammadiArani, O., Shavalipour, A., Moayedi, H. and Safarpour, H. (2021), "Frequency characteristics of a viscoelastic graphene nanoplatelet–reinforced composite circular microplate", *J. Vib. Control.*, **27**(1-2), 101-118. https://doi.org/10.1177/1077546320923930.

Ghazanfari, A., Soleimani, S.S., Keshavarzzadeh, M., Habibi, M., Assempuor, A. and Hashemi, R. (2020), "Prediction of FLD for sheet metal by considering through-thickness shear stresses", *Mech. Based Des. Struct.*, **48**(6), 755-772. https://doi.org/10.1080/15397734.2019.1662310.

Giesche, H. (1994), "Synthesis of monodispersed silica powders I. Particle properties and reaction kinetics", *J. Eur. Ceram. Soc.*, **14**(3), 189-204. https://doi.org/10.1016/0955-2219(94)90087-6.

Green, D.L., Lin, J.S., Lam, Y.F., Hu, M.Z.C., Schaefer, D.W. and Harris, M.T. (2003), "Size, volume fraction, and nucleation of Stober silica nanoparticles", *J. Colloid Interf. Sci.*, **266**(2), 346-358. https://doi.org/10.1016/s0021-9797(03)00610-6.

Guo, S. and Wang, E. (2011), "Functional micro/nanostructures: Simple synthesis and application in sensors, fuel cells, and gene delivery", *Accounts Chem. Res.*, **44**(7), 491-500. https://doi.org/10.1021/AR200001M.

Guo, J., Baharvand, A., Tazeddinova, D., Habibi, M., Safarpour, H., Roco-Videla, A. and Selmi, A. (2021a), "An intelligent computer method for vibration responses of the spinning multi-layer symmetric nanosystem using multi-physics modeling", *Eng. Comput.*, 1-22. https://doi.org/10.1007/s00366-021-01433-4.

Guo, Y., Mi, H. and Habibi, M. (2021b), "Electromechanical energy absorption, resonance frequency, and low-velocity impact analysis of the piezoelectric doubly curved system", *Mech. Syst. Signal Proc.*, **157**, 107723. https://doi.org/10.1016/j.ymssp.2021.107723.

Han, Y., Lu, Z., Teng, Z., Liang, J., Guo, Z., Wang, D., Han, M.Y. and Yang, W. (2017), "Unraveling the growth mechanism of silica particles in the Stöber method: In situ seeded growth model", *Langmuir*, **33**(23), 5879-5890. https://doi.org/10.1021/acs.langmuir.7b01140.

Harris, M.T., Brunson, R.R. and Byers, C.H. (1990), "The base-catalyzed hydrolysis and condensation reactions of dilute and concentrated TEOS solutions", *J. Non Cryst. Solids*, **121**(1), 397-403. https://doi.org/10.1016/0022-3093(90)90165-I.

Hashemi, H.R., Alizadeh, A.A., Oyarhossein, M.A., Shavalipour, A., Makkiabadi, M. and Habibi, M. (2021), "Influence of imperfection on amplitude and resonance frequency of a reinforcement compositionally graded nanostructure", *Wave. Random Complex Med.*, **31**(6), 1340-1366. https://doi.org/10.1080/17455030.2019.1662968.

He, S., Guo, F., Zou, Q. and Bioinformatics, H.J.C. (2020), "MRMD2.0: A python tool for machine learning with feature ranking and reduction", **15**, 1-9. http://doi.org/10.2174/1574893615999200503030350.

He, X., Ding, J., Habibi, M., Safarpour, H. and Safarpour, M. (2021), "Non-polynomial framework for bending responses of the multi-scale hybrid laminated nanocomposite reinforced circular/annular plate", *Thin Wall. Struct.*, **166**, 108019. https://doi.org/10.1016/j.tws.2021.108019.

Hiszpanski, A.M., Gallagher, B., Chellappan, K., Li, P., Liu, S., Kim, H., Han, J., Kailkhura, B., Buttler, D.J. and Han, T.Y. (2020), "Nanomaterial synthesis insights from machine learning of scientific articles by extracting, structuring, and visualizing knowledge", *J. Chem. Inf. Model.*, **60**(6), 2876-2887. https://doi.org/10.1021/acs.jcim.0c00199.

Hou, F., Wu, S., Moradi, Z. and Shafiei, N. (2021), "The computational modeling for the static analysis of axially functionally graded micro-cylindrical imperfect beam applying the computer simulation", *Eng. Comput.*, 1-19. https://doi.org/10.1007/s00366-021-01456-x.

Hu, J., Zhang, H., Li, Z., Zhao, C., Xu, Z. and Pan, Q. (2021), "Object traversing by monocular UAV in outdoor environment", *Asian J. Control.*, **23**(6), 2766-2775. https://doi.org/10.1002/asjc.2415.

Huang, X., Hao, H., Oslub, K., Habibi, M. and Tounsi, A. (2021a), "Dynamic stability/instability simulation of the rotary size-dependent functionally graded microsystem", *Eng. Comput.*, 1-17. https://doi.org/10.1007/s00366-021-01399-3.

Huang, X., Zhang, Y., Moradi, Z. and Shafiei, N. (2021b), "Computer simulation via a couple of homotopy perturbation methods and the generalized differential quadrature method for nonlinear vibration of functionally graded non-uniform micro-tube", *Eng. Comput.*, 1-18. https://doi.org/10.1007/s00366-021-01395-7.

Huang, X., Zhu, Y., Vafaei, P., Moradi, Z. and Davoudi, M. (2021c), "An iterative simulation algorithm for large oscillation of the applicable 2D-electrical system on a complex nonlinear substrate", *Eng. Comput.*, 1-13. https://doi.org/10.1007/s00366-021-01320-y.

Huo, J., Zhang, G., Ghabussi, A. and Habibi, M. (2021), "Bending analysis of FG-GPLRC axisymmetric circular/annular sector plates by considering elastic foundation and horizontal friction

force using 3D-poroelasticity theory", *Compos. Struct.*, **276**, 114438. https://doi.org/10.1016/j.compstruct.2021.114438.

Jiang, S., Dyk, A.V., Maurice, A., Bohling, J., Fasano, D. and Brownell, S. (2017), "Design colloidal particle morphology and self-assembly for coating applications", *Chem. Soc. Rev.*, **46**(12), 3792-3807. https://doi.org/10.1039/C6CS00807K.

Jiao, J., Ghoreishi, S.M., Moradi, Z. and Oslub, K. (2021), "Coupled particle swarm optimization method with genetic algorithm for the static–dynamic performance of the magneto-electro-elastic nanosystem", *Eng. Comput.*, 1-15. https://doi.org/10.1007/s00366-021-01391-x.

Jinnouchi, R. and Asahi, R. (2017), "Predicting catalytic activity of nanoparticles by a DFT-aided machine-learning algorithm", *J. Phys. Chem. Lett.*, **8**(17), 4279-4283. https://doi.org/10.1021/acs.jpclett.7b02010.

Khademolhosseini, R., Jafari, A., Mousavi, S.M. and Manteghian, M. (2019), "Investigation of synergistic effects between silica nanoparticles, biosurfactant and salinity in simultaneous flooding for enhanced oil recovery", *RSC Adv.*, **9**(35), 20281-20294. https://doi.org/10.1039/C9RA02039J.

Khezri, K., Saeedi, M. and Maleki Dizaj, S. (2018), "Application of nanoparticles in percutaneous delivery of active ingredients in cosmetic preparations", *Biomed. Pharmacother.*, **106** 1499-1505. https://doi.org/10.1016/J.BIOPHA.2018.07.084.

Kim, J.W., Kim, L.U. and Kim, C.K. (2007), "Size control of silica nanoparticles and their surface treatment for fabrication of dental nanocomposites", *Biomacromolecules*, **8**(1), 215-222. https://doi.org/10.1021/bm060560b.

Kim, S. and Zukoski, C.F. (1990), "A model of growth by hetero-coagulation in seeded colloidal dispersions", *J. Colloid Interf. Sci.*, **139**(1), 198-212. https://doi.org/10.1016/0021-9797(90)90457-Y.

Klemperer, W.G., Mainz, V.V. and Millar, D.M. (1986), "A solid state multinuclear magnetic resonance study of the sol-gel process using polysilicate precursors", *MRS Online Proceedings Library*, **73**(1), 15-25. https://doi.org/10.1557/PROC-73-15.

Kumar, Y., Gupta, A. and Tounsi, A. (2021), "Size-dependent vibration response of porous graded nanostructure with FEM and nonlocal continuum model", *Adv Nano Res.* **11**(1), 1-17. https://doi.org/10.12989/anr.2021.11.1.001.

LaMer, V.K. and Dinegar, R.H. (1950), "Theory, production and mechanism of formation of monodispersed hydrosols", *J. Am. Chem. Soc.*, **72**(11), 4847-4854. https://doi.org/10.1021/ja01167a0011.

Lee, K., Look, J.L., Harris, M.T. and McCormick, A.V. (1997), "Assessing extreme models of the Stöber synthesis using transients under a range of initial composition", *J. Colloid Interf. Sci.*, **194**(1), 78-88. https://doi.org/10.1006/jcis.1997.5089.

Lee, K., Sathyagal, A.N. and McCormick, A.V. (1998), "A closer look at an aggregation model of the Stöber process", *Colloid Surfaces A*, **144**(1), 115-125. https://doi.org/10.1016/S0927-7757(98)00566-4.

Li, B., Xiao, G., Lu, R., Deng, R. and Bao, H. (2020a), "On feasibility and limitations of detecting false data injection attacks on power grid state estimation using D-facts devices", *IEEE T. Ind. Inform.*, **16**(2), 854-864. https://doi.org/10.1109/TII.2019.2922215.

Li, J., Tang, F. and Habibi, M. (2020b), "Bi-directional thermal buckling and resonance frequency characteristics of a GNP-reinforced composite nanostructure", *Eng. Comput.*, 1-22. https://doi.org/10.1007/s00366-020-01110-y.

Li, Y., Li, S., Guo, K., Fang, X. and Habibi, M. (2020c), "On the modeling of bending responses of graphene-reinforced higher order annular plate via two-dimensional continuum mechanics approach", *Eng. Comput.*, 1-22. https://doi.org/10.1007/s00366-020-01166-w.

Li, Y., Macdonald, D.D., Yang, J., Qiu, J. and Wang, S. (2020d), "Point defect model for the corrosion of steels in supercritical water: Part I, film growth kinetics", *Corros. Sci.*, **163**, 108280. https://doi.org/10.1016/j.corsci.2019.108280.

Liu, J., Qiao, S. Z., Liu, H., Chen, J., Orpe, A., Zhao, D. and Lu, G.Q. (2011), "Extension of the Stöber method to the preparation of monodisperse resorcinol-formaldehyde resin polymer and carbon spheres", *Angewandte Chemie*, **50**(26), 5947-5951. https://doi.org/10.1002/ANIE.201102011.

Liu, H., Shen, S., Oslub, K., Habibi, M. and Safarpour, H. (2021a), "Amplitude motion and frequency simulation of a composite viscoelastic microsystem within modified couple stress elasticity", *Eng. Comput.*, 1-15. https://doi.org/10.1007/s00366-021-01316-8.

Liu, H., Zhao, Y., Pishbin, M., Habibi, M., Bashir, M.O. and Issakhov, A. (2021b), "A comprehensive mathematical simulation of the composite size-dependent rotary 3D microsystem via two-dimensional generalized differential quadrature method", *Eng. Comput.*, 1-16. https://doi.org/10.1007/s00366-021-01419-2.

Liu, Y., Wang, W., He, T., Moradi, Z. and Larco Benítez, M.A. (2021c), "On the modelling of the vibration behaviors via discrete singular convolution method for a high-order sector annular system", *Eng. Comput.*, 1-23. https://doi.org/10.1007/s00366-021-01454-z.

Liu, Z., Su, S., Xi, D. and Habibi, M. (2020a), "Vibrational responses of a MHC viscoelastic thick annular plate in thermal environment using GDQ method", *Mech. Based Des. Struct.*, 1-26. https://doi.org/10.1080/15397734.2020.1784201.

Liu, Z., Wu, X., Yu, M. and Habibi, M. (2020b), "Large-amplitude dynamical behavior of multilayer graphene platelets reinforced nanocomposite annular plate under thermo-mechanical loadings", *Mech. Based Des. Struct.*, 1-25. https://doi.org/10.1080/15397734.2020.1815544.

Ma, L., Liu, X. and Moradi, Z. (2021a), "On the chaotic behavior of graphene-reinforced annular systems under harmonic excitation", *Eng. Comput.*, 1-25. https://doi.org/10.1007/s00366-020-01210-9.

Ma, Z., Zheng, W., Chen, X. and Yin, L. (2021b), "Joint embedding VQA model based on dynamic word vector", *Peer J. Comput. Sci.*, **7**, e353. https://doi.org/10.7717/peerj-cs.353.

Matsoukas, T. and Gulari, E. (1988), "Dynamics of growth of silica particles from ammonia-catalyzed hydrolysis of tetra-ethyl-orthosilicate", *J. Colloid Interf. Sci.*, **124**(1), 252-261. https://doi.org/10.1016/0021-9797(88)90346-3.

Moayedi, H., Aliakbarlou, H., Jebeli, M., Noormohammadiarani, O., Habibi, M., Safarpour, H. and Foong, L.K. (2020a), "Thermal buckling responses of a graphene reinforced composite micropanel structure", *Int. J. Appl. Mech.*, **12**(1), 2050010. https://doi.org/10.1142/s1758825120500106.

Moayedi, H., Darabi, R., Ghabussi, A., Habibi, M. and Foong, L.K. (2020b), "Weld orientation effects on the formability of tailor welded thin steel sheets", *Thin Wall. Struct.*, **149**, 106669. https://doi.org/10.1016/j.tws.2020.106669.

Moayedi, H., Ebrahimi, F., Habibi, M., Safarpour, H. and Foong, L.K. (2021), "Application of nonlocal strain–stress gradient theory and GDQEM for thermo-vibration responses of a laminated composite nanoshell", *Eng. Comput.*, **37**(4), 3359-3374. https://doi.org/10.1007/s00366-020-01002-1.

Moradi, Z., Davoudi, M., Ebrahimi, F. and Ehyaei, A.F. (2021), "Intelligent wave dispersion control of an inhomogeneous micro-shell using a proportional-derivative smart controller", *Wave. Random Complex Med.*, 1-24. https://doi.org/10.1080/17455030.2021.1926572.

Najaafi, N., Jamali, M., Habibi, M., Sadeghi, S., Jung, D.W. and Nabipour, N. (2021), "Dynamic instability responses of the substructure living biological cells in the cytoplasm

environment using stress-strain size-dependent theory", *J. Biomol. Struct. Dyn.*, **39**(7), 2543-2554. https://doi.org/10.1080/07391102.2020.1751297.

Nezadi, M., Keshvari, H. and Yousefzadeh, M. (2021), "Using Taguchi design of experiments for the optimization of electrospun thermoplastic polyurethane scaffolds", *Adv. Nano Res.*, **10**(1), 59-69. https://doi.org/10.12989/anr.2021.10.1.059.

Oyarhossein, M.A., Alizadeh, A.A., Habibi, M., Makkiabadi, M., Daman, M., Safarpour, H. and Jung, D.W. (2020), "Dynamic response of the nonlocal strain-stress gradient in laminated polymer composites microtubes", *Sci. Rep.*, **10**(1), 5616. https://doi.org/10.1038/s41598-020-61855-w.

Peng, D., Chen, S., Darabi, R., Ghabussi, A. and Habibi, M. (2021), "Prediction of the bending and out-of-plane loading effects on formability response of the steel sheets", *Arch. Civil Mech. Eng.*, **21**(2), 74. https://doi.org/10.1007/s43452-021-00227-1.

Polte, J. (2015), "Fundamental growth principles of colloidal metal nanoparticles – a new perspective", *Cryst. Eng. Comm.*, **17**(36), 6809-6830. https://doi.org/10.1039/C5CE01014D.

Prabha, S., Durgalakshmi, D., Rajendran, S. and Lichtfouse, E. (2021), "Plant-derived silica nanoparticles and composites for biosensors, bioimaging, drug delivery and supercapacitors: A review", *Environ. Chem. Lett.*, **19**(2), 1667-1691. https://doi.org/10.1007/S10311-020-01123-5.

Qiao, G., Ding, L., Zhang, L. and Yan, H. (2021), "Accessible tourism: A bibliometric review (2008–2020)", *Tourism Review*. https://doi.org/10.1108/TR-12-2020-0619.

Rahman, I.A., Vejayakumaran, P., Sipaut, C.S., Ismail, J., Bakar, M.A., Adnan, R. and Chee, C.K. (2007), "An optimized sol–gel synthesis of stable primary equivalent silica particles", *Colloid Surfaces A*, **1-3**(294), 102-110. https://doi.org/10.1016/J.COLSURFA.2006.08.001.

Rao, K.S., El-Hami, K., Kodaki, T., Matsushige, K. and Makino, K. (2005), "A novel method for synthesis of silica nanoparticles", *J. Colloid. Interf. Sci.*, **289**(1), 125-131. https://doi.org/10.1016/j.jcis.2005.02.019.

Shah, A.H. and Rather, M.A. (2021), "Pharmaceutical residues: New emerging contaminants and their mitigation by nano-photocatalysis", *Adv. Nano Res.*, **10**(4), 397-414. https://doi.org/10.12989/anr.2021.10.4.397.

Shao, Y., Zhao, Y., Gao, J. and Habibi, M. (2021), "Energy absorption of the strengthened viscoelastic multi-curved composite panel under friction force", *Arch. Civil Mech. Eng.*, **21**(4), 141. https://doi.org/10.1007/s43452-021-00279-3.

Shariati, A., Jung, D.W., Mohammad-Sedighi, H., Żur, K.K., Habibi, M. and Safa, M. (2020), "Stability and dynamics of viscoelastic moving rayleigh beams with an asymmetrical distribution of material parameters", *Symmetry*, **12**(4), 586. https://doi.org/10.3390/sym12040586.

Shariati, A., Habibi, M., Tounsi, A., Safarpour, H. and Safa, M. (2021), "Application of exact continuum size-dependent theory for stability and frequency analysis of a curved cantilevered microtubule by considering viscoelastic properties", *Eng. Comput.*, **37**(4), 3629-3648. https://doi.org/10.1007/s00366-020-01024-9.

Shi, X., Li, J. and Habibi, M. (2020), "On the statics and dynamics of an electro-thermo-mechanically porous GPLRC nanoshell conveying fluid flow", *Mech. Based Des. Struct.*, 1-37. https://doi.org/10.1080/15397734.2020.1772088.

Stöber, W., Fink, A. and Bohn, E. (1968), "Controlled growth of monodisperse silica spheres in the micron size range", *J. Colloid Interf. Sci.*, **26**(1), 62-69. https://doi.org/10.1016/0021-9797(68)90272-5.

Sun, J., Wang, Y., Liu, S., Dehghani, A., Xiang, X., Wei, J. and Wang, X. (2021), "Mechanical, chemical and hydrothermal activation for waste glass reinforced cement", *Constr. Build. Mater.*, **301**, 124361. https://doi.org/10.1016/j.conbuildmat.2021.124361.

Svirbely, W.J. and Mador, I.L. (1950), "Kinetics of the alkaline hydrolysis of monoethyl malonate ion", *J. Am. Chem. Soc.*, **72**(12), 5699-5705. https://doi.org/10.1021/JA01168A089.

Tan, C.G., Bowen, B.D. and Epstein, N. (1987), "Production of monodisperse colloidal silica spheres: Effect of temperature", *J. Colloid Interf. Sci.*, **118**(1), 290-293. https://doi.org/10.1016/0021-9797(87)90458-9.

Tian, H., Wang, T., Zhang, F., Zhao, S., Wan, S., He, F. and Wang, G. (2018), "Tunable porous carbon spheres for high-performance rechargeable batteries", *J. Mater. Chem. A.*, **6**(27), 12816-12841. https://doi.org/10.1039/C8TA02353K.

Ways, M.T.M., Ng, K.W., Lau, W.M. and Khutoryanskiy, V.V. (2020), "Silica nanoparticles in transmucosal drug delivery", *Pharmaceutics*, **12**(8), 1-25. https://doi.org/10.3390/pharmaceutics12080751.

van Blaaderen, A. and Kentgens, A.P.M. (1992), "Particle morphology and chemical microstructure of colloidal silica spheres made from alkoxysilanes", *J. Non Cryst. Solid.*, **149**(3), 161-178. https://doi.org/10.1016/0022-3093(92)90064-q.

van Blaaderen, A., Van Geest, J. and Vrij, A. (1992), "Monodisperse colloidal silica spheres from tetraalkoxysilanes: Particle formation and growth mechanism", *J. Colloid Interf. Sci.*, **154**(2), 481-501. https://doi.org/10.1016/0021-9797(92)90163-g.

van Helden, A.K., Jansen, J.W. and Vrij, A. (1981), "Preparation and characterization of spherical monodisperse silica dispersions in nonaqueous solvents", *J. Colloid Interf. Sci.*, **81**(2), 354-368. https://doi.org/10.1016/0021-9797(81)90417-3.

Wang, T., Liu, W., Zhao, J., Guo, X. and Terzija, V. (2020a), "A rough set-based bio-inspired fault diagnosis method for electrical substations", *Int. J. Electr. Power.*, **119**, 105961. https://doi.org/10.1016/j.ijepes.2020.105961.

Wang, Z., Yu, S., Xiao, Z. and Habibi, M. (2020b), "Frequency and buckling responses of a high-speed rotating fiber metal laminated cantilevered microdisk", *Mech. Adv. Mater. Struct.*, 1-14. https://doi.org/10.1080/15376494.2020.1824284.

Wu, J. and Habibi, M. (2021), "Dynamic simulation of the ultra-fast-rotating sandwich cantilever disk via finite element and semi-numerical methods", *Eng. Comput.*, 1-17. https://doi.org/10.1007/s00366-021-01396-6.

Xiong, Q.M., Chen, Z., Huang, J.T., Zhang, M., Song, H., Hou, X.F., Li, X.B. and Feng, Z.J. (2020), "Preparation, structure and mechanical properties of Sialon ceramics by transition metal-catalyzed nitriding reaction", *Rare Metals.* **39**(5), 589-596. https://doi.org/10.1007/s12598-020-01385-6.

Xu, W., Pan, G., Moradi, Z. and Shafiei, N. (2021), "Nonlinear forced vibration analysis of functionally graded non-uniform cylindrical microbeams applying the semi-analytical solution", *Compos. Struct.*, **275**, 114395. https://doi.org/10.1016/j.compstruct.2021.114395.

Xu, X., Wang, C. and Zhou, P. (2021), "GVRP considered oil-gas recovery in refined oil distribution: From an environmental perspective", *Int. J. Prod. Econ.*, **235**, 108078. http://doi.org/10.1016/j.ijpe.2021.108078.

Yang, X., Liu, X., Zhang, A., Lu, D., Li, G., Zhang, Q., Liu, Q. and Jiang, G. (2019), "Distinguishing the sources of silica nanoparticles by dual isotopic fingerprinting and machine learning", *Nature Commun.*, **10**(1), 1-9. https://doi.org/10.1038/s41467-019-09629-5.

Yu, X., Maalla, A. and Moradi, Z. (2022), "Electroelastic high-order computational continuum strategy for critical voltage and frequency of piezoelectric NEMS via modified multi-physical couple stress theory", *Mech. Syst. Signal Proc.*, **165**, 108373. https://doi.org/10.1016/j.ymssp.2021.108373.

Zhang, X., Tang, Y., Zhang, F. and Lee, C.S. (2016), "A novel

aluminum–graphite dual-ion battery", *Adv. Energy Mater.*, **6**(11), 1502588. https://doi.org/10.1002/aenm.201502588.

Zhang, L., Chen, Z., Habibi, M., Ghabussi, A. and Alyousef, R. (2021a), "Low-velocity impact, resonance, and frequency responses of FG-GPLRC viscoelastic doubly curved panel", *Compos. Struct.*, **269**, 114000. https://doi.org/10.1016/j.compstruct.2021.114000.

Zhang, X., Shamsodin, M., Wang, H., NoormohammadiArani, O., Khan, A.M., Habibi, M. and Al-Furjan, M.S.H. (2021b), "Dynamic information of the time-dependent tobullian biomolecular structure using a high-accuracy size-dependent theory", *J. Biomol. Struct. Dyn.*, **39**(9), 3128-3143. https://doi.org/10.1080/07391102.2020.1760939.

Zhang, Y., Wang, Z., Tazeddinova, D., Ebrahimi, F., Habibi, M. and Safarpour, H. (2021c), "Enhancing active vibration control performances in a smart rotary sandwich thick nanostructure conveying viscous fluid flow by a PD controller", *Wave. Random Complex Med.*, 1-24. https://doi.org/10.1080/17455030.2021.1948627.

Zhang, T., Wu, X., Shaheen, S.M., Abdelrahman, H., Ali, E.F., Bolan, N.S., Ok, Y.S., Li, G., Tsang, D.C.W. and Rinklebe, J. (2022), "Improving the humification and phosphorus flow during swine manure composting: A trial for enhancing the beneficial applications of hazardous biowastes", *J. Hazard. Mater.*, **425**, 127906. https://doi.org/10.1016/j.jhazmat.2021.127906.

Zhao, Y., Moradi, Z., Davoudi, M. and Zhuang, J. (2021), "Bending and stress responses of the hybrid axisymmetric system via state-space method and 3D-elasticity theory", *Eng. Comput.*, 1-23. https://doi.org/10.1007/s00366-020-01242-1.

Zhou, C., Zhao, Y., Zhang, J., Fang, Y. and Habibi, M. (2020), "Vibrational characteristics of multi-phase nanocomposite reinforced circular/annular system", *Adv. Nano Res.*, **9**(4), 295-295. https://doi.org/10.12989/ANR.2020.9.4.295.

Zhu, H., Zhu, J., Zhang, Z. and Zhao, R. (2021), "Crossover from linear chains to a honeycomb network for the nucleation of hexagonal boron nitride grown on the Ni(111) surface", *J. Phys. Chem. C*, **125**(48), 26542-26551. https://doi.org/10.1021/acs.jpcc.1c09334.

SR